Journal of the Ceramic Society of Japan 103 [5] 444-448 (1995)

Paper

Kinetics of Remelting Reaction in Ca_2SiO_4 Solid Solutions

Koichiro FUKUDA, Iwao MAKI, Suketoshi ITO and Kazuhiro TOYODA*

Department of Materials Science and Engineering, Nagoya Institute of Technology, Gokiso-cho, Showa-ku, Nagoya 466
**Graduate School of Science, The University of Tokyo, 7-1-3, Hongo, Bunkyo-ku, Tokyo 113*

Ca_2SiO_4 固溶体における再融反応の速度論

福田功一郎・牧　巖・伊藤祐敏・豊田和弘*

名古屋工業大学材料工学科，466 愛知県名古屋市昭和区御器所町
*東京大学大学院理学系研究科鉱物学専攻，113 東京都文京区本郷 7-1-3

[Received November 21, 1994; Accepted February 21, 1995]

The cell dimensions for a series of β-Ca_2SiO_4 solid solutions were determined as a function of concentration of foreign oxides (Na_2O, Al_2O_3 and Fe_2O_3). The angle β varied most sensitively with the Na/(Na+Ca) ratio ($=x$) according to β (°) $=94.55-8.86\,x$ ($0\leq x\leq 0.03$). The decrease in x that accompanies the remelting reaction was therefore detectable by the increase in β. When the crystals were cooled at a constant rate r (°C/s) over the temperature range in which the remelting reaction occurred, the fraction remelted was expressed by $1-\exp(-1.33\,r^{-0.25})$.

Key-words : *Ca_2SiO_4, Solid solutions, Belite, Remelting reaction, Kinetics, Cell dimensions*

1. Introduction

The Ca_2SiO_4 (C_2S) polymorphs established so far are, at ordinary pressures, α, α'_H, α'_L and γ in the order of decreasing temperature.[1] The β phase, stable at high pressures, occurs metastably on rapid cooling. The polymorphic sequence and the crystal structures of Ca_2SiO_4 solid solution (C_2S(ss)) or belite in cement clinkers are considered to be analogous to those of pure C_2S. The α-to-α'_H transition of C_2S(ss) is a nucleation and growth process and can be represented on a time-temperature-transformation (TTT) diagram.[2] The α'_H phase is further inverted into the β phase passing through the α'_L phase. At ambient temperature C_2S(ss) consists of the α and/or the β phases depending on cooling rates as well as initial chemical compositions.

When cooled slowly, α-C_2S(ss) with plenty of foreign oxides in solid solution undergoes remelting reaction within the crystals after the transition to α'_H.[2)-5)] In this reaction the α'_H phase, consisting of six sets of lamellae,[6),7)] is separated into a liquid exsolved heterogeneously on the lamella boundaries and a new α'_H phase lower in impurity concentration. Fukuda et al.[4] explicated the decomposition process by following a series of changes in microtexture. The rate of decomposition depends on the physical properties of the exsolved liquid (e.g., wettability) as well as on temperature. The crystals with Al/Fe$>$1 produce liquids as readily spread on the lamellae and lead to a high rate of decomposition, whereas those with Al/Fe$<$1 produce liquid droplets on the lamella boundaries and are low in the rate of decomposition.[5]

In this study we prepared a series of β-C_2S(ss) with varying Na/(Na+Ca) ratios and determined their accurate cell dimensions. The angle β has been proved to provide a good indicator to show the progress of remelting reaction with cooling.

2. Experimental

2.1 Materials

Using regent-grade chemicals, pure C_2S and five kinds of C_2S(ss) doped with Na_2O, Al_2O_3 and Fe_2O_3 were prepared (Table 1). The mixtures were pressed into pellets, heated at 1500°C for 15 min and quenched in cold water. The specimens thus prepared were termed S-1 (pure C_2S) 2, 3, 4, 5 and 6 in the order of increasing concentration of foreign oxides. The C_2S(ss) crystals coexisted with a small amount of interstitial materials consisting mainly of calcium aluminate.

S-5 and S-6 were reheated at 1500°C for 5 min and cooled in three different ways: (A) quenching in air at 1500°C (S-5-A and S-6-A), (B) cooling at 1°C/s followed by quenching at 1000°C in air (S-5-B and S-6-B) and (C) cooling at 80°C/h followed by quenching at 1000°C in air (S-5-C and S-6-C).

2.2 Characterization

Thin and polished sections were prepared for all the samples and their microtextures were observed under an optical microscope.

The phase constitution of the crystals was examined by X-ray powder diffractometry (XRD). The profile data were collected on a diffractometer

Table 1. Preparation of Mixtures (mass%)

Sample	$CaCO_3$	SiO_2	$NaHCO_3$	Al_2O_3	Fe_2O_3
S-1	76.92	23.08			
S-2	76.18	22.86	0.74	0.11	0.11
S-3	76.18	21.97	1.42	0.22	0.22
S-4	75.49	21.76	2.10	0.32	0.32
S-5	74.80	21.57	2.78	0.43	0.43
S-6	72.18	20.81	5.37	0.82	0.82

(Model PW3050, Philips Co.) using monochromatized Cu Kα radiation (40 kV, 50 mA) and step-scan technique (step width=0.02° and fixed time=10 s) in the 2θ range from 20° to 57.7°. Si powder was used as an internal standard (sample/Si=7 by weight). The cell dimensions of the β phase for each specimen were refined by the WPPD (whole-powder-pattern decomposition without reference to a structural model) method.[8]

The compositions of C_2S(ss) in S-2, 3, 4, 5 and 6 were determined by chemical analysis. The crystals were separated by dissolving the interstitial materials with an aqueous solution of KOH and saccharose at 90°C. After alkali-fusion with Na_2CO_3, the SiO_2 content was determined gravimetrically from the loss in weight by treating one part of each sample with HF. The other part was acid-digested and the filtrate was used for analyzing Al, Ca and Fe with an inductively coupled plasma atomic emission spectrometer (ICP : Model JY48P(V), Seiko Co.) and Na with an atomic emission spectrometer (Model SAS-720, Seiko Co.).

3. Results and discussion

3.1 Constituent phases, chemical composition and microtextures

Both optical microscopy and XRD showed that at ambient temperature the crystals in S-6 were composed exclusively of the α phase and those in S-1, 2, 3, 4 and 5 of the β phase. On rapid cooling, no compositional change occurred during the successive transitions $\alpha \rightarrow \alpha'_H \rightarrow \alpha'_L \rightarrow \beta$. The chemical compositions of those crystals are given in Table 2. From the substitution scheme in the previous papers,[5),9)] it is probable that Al and Fe substitute for Si and Na for Ca. The chemical formulae have been derived assuming Ca+Na=2 (Table 2). The Si sites were almost filled with 1 to 5 % of the oxygen sites being vacant.

Thin-section microscopy showed that the crystals in S-6-A were composed mainly of the α phase as host with a very small amount of the β-phase lamellae. The TTT diagram was prepared in our previous study for the α-to-α'_H transition of the crystals in S-6 (Fig. 1).[2)] At 30°C/s the cooling curve just passes through the nose of the C-shaped curve for the start of transition. This cooling leads to the relevant

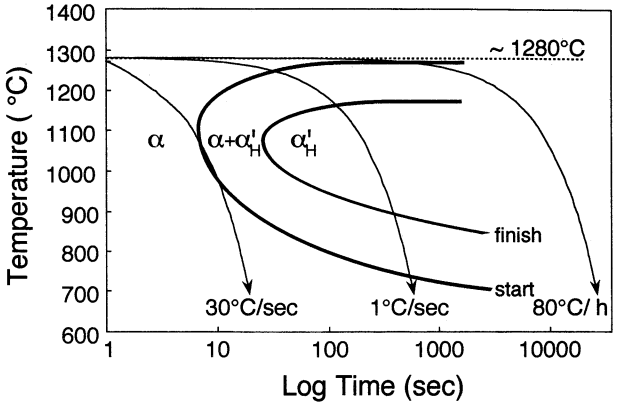

Fig. 1. Time-temperature-transformation diagram for the α-to-α'_H transition of C_2S(ss) in S-6.[2)] The thermodynamic transition temperature between α and α'_H is 1280°C. Curves for cooling at 30°C/s, 1°C/s and 80°C/h are superposed on the diagram.

microtexture and phase constitution of the crystals in S-6-A. The same cooling rate (30°C/s) is also expected for S-5-A, which was cooled in the same way as S-6-A. With decreasing concentration of foreign oxides in solid solution, both curves for the start and finish of transition may shift toward left in the diagram.[2)] Because the crystals in S-5-A were composed entirely of the β phase, the TTT diagram for the crystals in S-5 should be such that the cooling curve for 30°C/s crosses both curves.

All the crystals in S-5-B, S-6-B, S-5-C and S-6-C were composed of the β phase. The occurrence of the remelting reaction was confirmed microscopically within those crystals. Because the Al/Fe ratio in their parent crystals is larger than 1 (Table 2), the remelting reaction should proceed to its final stage with prolonged heat treatment as suggested by Fukuda et al.[5)]

3.2 Dependence of cell dimensions on Na/(Na+Ca) ratio

All the refined cell dimensions of the β phase are given in Table 3 together with final reliability factors. In Fig. 2 the cell dimensions are plotted against Na/(Na+Ca) ratios ($=x$). With increasing x the a-axis shrank while the b- and c-axis expanded with eventual increase in the unit-cell volume. The angle β decreased, showing the best correlation with x as

Table 2. Chemical Composition and Formula of the C_2S(ss)

Sample	Chemical Composition (mass%)						Chemical Formula	Na/(Na+Ca)	Al/Fe
	CaO	SiO_2	Na_2O	Al_2O_3	Fe_2O_3	Total			
S-2	64.6	34.2	0.38	0.12	0.13	99.4	$(Ca_{1.98}Na_{0.02})_{\Sigma 2}(Si_{0.98}Al_{0.004}Fe_{0.003})_{\Sigma 0.99}O_{3.96}$	0.01	1.4
S-3	64.9	33.7	0.53	0.32	0.25	99.7	$(Ca_{1.97}Na_{0.03})_{\Sigma 2}(Si_{0.96}Al_{0.01}Fe_{0.01})_{\Sigma 0.97}O_{3.92}$	0.015	2.0
S-4	64.0	33.5	0.89	0.44	0.42	99.3	$(Ca_{1.95}Na_{0.05})_{\Sigma 2}(Si_{0.95}Al_{0.02}Fe_{0.01})_{\Sigma 0.98}O_{3.92}$	0.025	1.6
S-5	63.9	33.4	1.01	0.76	0.55	99.6	$(Ca_{1.94}Na_{0.06})_{\Sigma 2}(Si_{0.95}Al_{0.03}Fe_{0.01})_{\Sigma 0.99}O_{3.93}$	0.03	2.2
S-6	62.0	31.8	2.38	1.20	1.20	98.6	$(Ca_{1.87}Na_{0.13})_{\Sigma 2}(Si_{0.90}Al_{0.04}Fe_{0.03})_{\Sigma 0.96}O_{3.82}$	0.065	1.6

Table 3. Cell Dimensions for the β-C_2S(ss)

Sample	Cell dimensions					Reliability factors*		
	a (nm)	b (nm)	c (nm)	β (°)	Volume (nm^3)	R_p	R_{wp}	R_p(peak)
S-1	0.55089(1)	0.67536(1)	0.93102(2)	94.552(2)	0.34529(2)	0.0388	0.0529	0.0617
S-2	0.55063(1)	0.67571(2)	0.93142(3)	94.465(3)	0.34550(3)	0.0382	0.0531	0.0609
S-3	0.55040(2)	0.67593(3)	0.93232(4)	94.415(4)	0.34582(5)	0.0405	0.0579	0.0661
S-4	0.55023(3)	0.67602(3)	0.93274(5)	94.337(4)	0.34595(6)	0.0465	0.0664	0.0762
S-5	0.54985(3)	0.67603(4)	0.93361(10)	94.282(8)	0.34606(9)	0.0490	0.0699	0.0885
S-5-A	0.55029(3)	0.67582(3)	0.93261(6)	94.396(5)	0.34581(6)	0.0460	0.0642	0.0806
S-5-B	0.55056(2)	0.67550(2)	0.93167(4)	94.494(3)	0.34543(3)	0.0425	0.0611	0.0739
S-5-C	0.55084(1)	0.67540(2)	0.93132(3)	94.550(3)	0.34539(3)	0.0439	0.0606	0.0786
S-6-B	0.55042(3)	0.67557(3)	0.93226(6)	94.422(5)	0.34563(5)	0.0402	0.0555	0.0789
S-6-C	0.55072(2)	0.67548(3)	0.93169(4)	94.526(4)	0.34551(4)	0.0451	0.0616	0.0900

Figures in parentheses indicate standard deviations.

*Reliability factors were calculated by

$R_p = \Sigma \mid y(obs)_i - y(calc)_i \mid / \Sigma\, y(obs)_i$

$R_{wp} = [\Sigma w_i[y(obs)_i - y(calc)_i]^2 / \Sigma\, w_i\, y(obs)_i^{\,2}]^{1/2}$

$R_p(peak) = \Sigma \mid y(obs)_i - y(calc)_i \mid / \Sigma\, [y(obs)_i - b(calc)_i]$

where $y(obs)_i$ and $y(calc)_i$ are respectively ith observed and calculated profile intensities and w_i is a weight assigned to the observed intensity in the form $w_i = y(obs)_i^{-1}$. $b(calc)_i$ is a calculated background intensity.

shown in Fig. 2(D). The Al and Fe had no appreciable effect on the change in cell dimensions. These are very similar to the result given by Turnock et al.[10] for monoclinic pyroxene $(Ca_xMg_yFe_{1-x-y})SiO_3$, in which the angle β changed sensitively with Ca/(Ca+Mg+Fe) ratios.

The relation between β and x for the β-phase crystals in S-1, 2, 3, 4 and 5 is given by

$$\beta(°) = 94.55 - 8.86x \quad (R = 0.999) \qquad (1)$$

This equation holds when $0 \leq x \leq 0.03$.

It should be noted that, with the remelted crystals, the x values in Fig. 2 are for their parent crystals before remelting. The Na/(Na+Ca) ratio is hereafter denoted by x_p. The three broken lines in Fig. 2(D) relate the x_p to β as follows:

$$\beta(°) = 94.55 - S(r)x_p \qquad (2)$$

where $S(r)$ is the slope of the line for the constant cooling rate r. The values of $S(r)$ for different r are given in Table 4.

Table 4. Examples of S and ζ Values as a Function of Linear Cooling Rate r

r	30°/sec	1°/sec	80°/h
S	5.20	1.99	0.34
ζ	0.41	0.78	0.96

3.3 Compositional change induced by the remelting reaction

During the remelting reaction, the impurity concentration in the parent crystals continues to

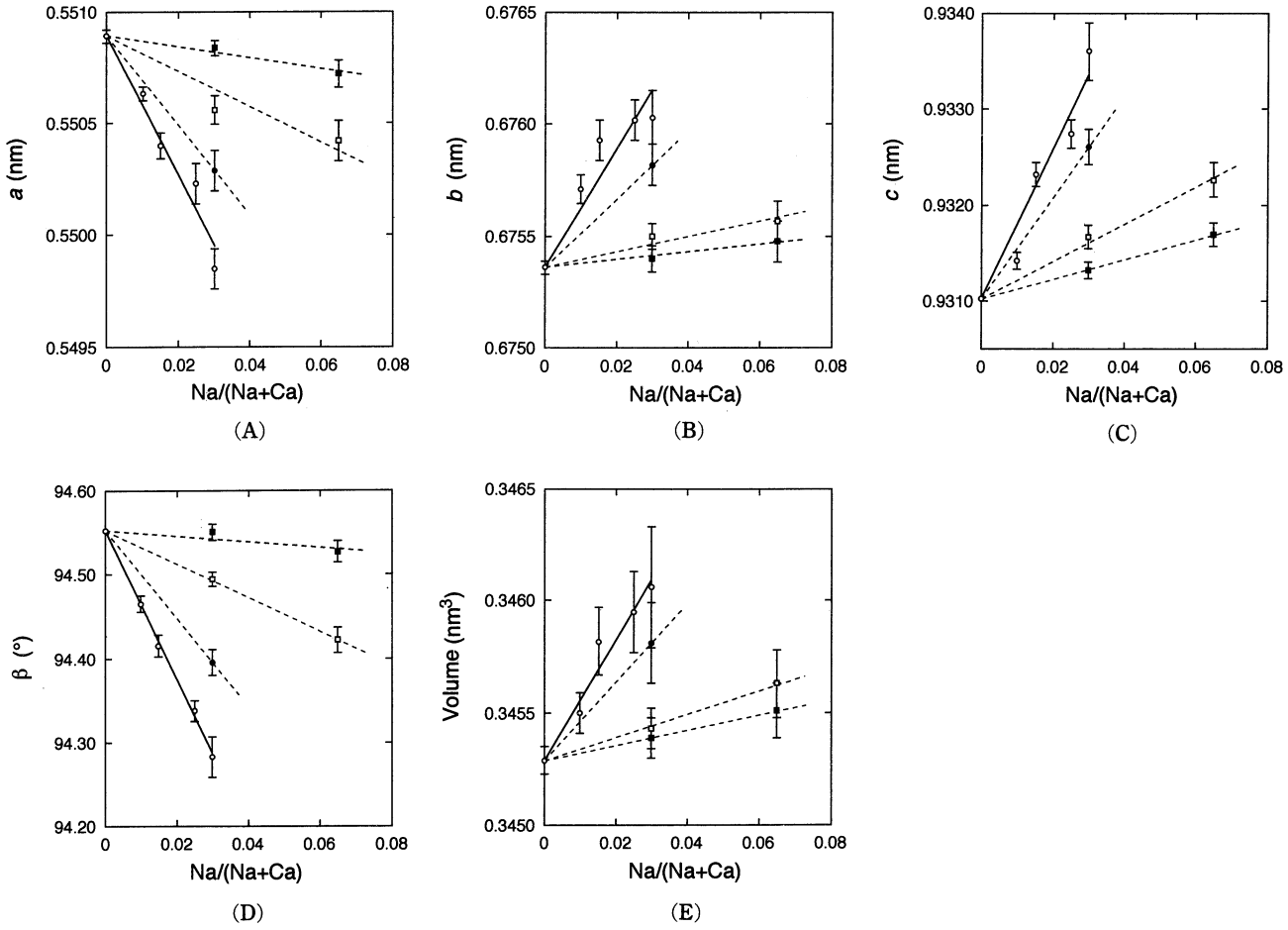

Fig. 2. Variation of cell dimensions with Na/(Na+Ca) ratio. a (A), b (B), c (C), β (D) and volume (E). Quenched at 1500°C (○). Cooled at 30°/s (●), 1°/s (□) and 80°/h (■). Error bars indicate 3 σ. The Na/(Na+Ca) ratios for ●, □ and ■ are those of the parent crystals before the occurrence of the remelting reaction.

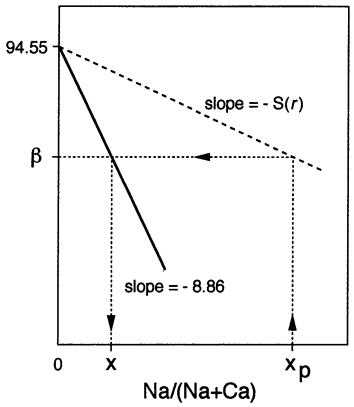

Fig. 3. Schematic illustration for determining the actual Na/(Na+Ca) ratio from the angle β after remelting reaction. Na/(Na+Ca) ratio decreases from x_p to x.

decrease.[3),4)] Figure 3 shows schematically the relation between x_p and x in the decomposed C_2S(ss) crystals, which can be derived from Eqs. (1) and (2) as

$$x=[S(r)/8.86]x_p \quad (3)$$

Because the $S(r)$ values are smaller than 8.86, the x values are smaller than the corresponding x_p values. For example, with $x_p=0.03$, x is 0.018 for $r=30$℃/s, 0.007 for $r=1$℃/s and 0.001 for $r=80$℃/h.

The fraction remelted (ζ) can be defined by

$$\zeta=(x_p-x)/(x_p-x_f) \quad (4)$$

where x_f is the final Na/(Na+Ca) ratio of the completely remelted crystal. The ζ value is 0 at the beginning of the reaction ($x=x_p$) and 1 at the end ($x=x_f$). Supposing that the completely remelted crystal is free from impurities ($x_f=0$), substitution of Eq. (3) into Eq. (4) gives

$$\zeta=1-S(r)/8.86 \quad (5)$$

Table 4 gives ζ values in terms of r and S.

3.4 Kinetics of the remelting reaction during cooling

The kinetics for a wide range of mineral reactions under isothermal conditions can be represented by the Avrami equation.[11)-13)] The following equation is expected to hold for the present remelting reaction.

$$\zeta=1-\exp(-kt^n) \quad (6)$$

where t is time, k is a rate constant which depends on temperature and n is an empirical parameter related to the reaction mechanism. From Eq. (6), the derivative of ζ with respect to t is

$$d\zeta/dt=nk(1-\zeta)t^{n-1} \quad (7)$$

With cooling at a constant rate r, temperature (T) and time (t) are related by

$$T=T_i-rt \quad (8)$$

where T_i is the initial temperature at which the remelting reaction starts. Substitution of Eq. (8) into Eq. (7), separation of the variables and integration of both sides give

$$r^n\int_0^{\zeta}(1-\zeta)^{-1}\,d\zeta = -n\int_{T_i}^{T_f}k(T_i-T)^{n-1}\,dT \quad (9)$$

where T_f is the final temperature below which the remelting reaction no longer occurs. Because the reaction mechanism is supposed unchanged between T_i and T_f, n should have a constant value. Replacement of the right side of Eq. (9) by a constant C and the solution of the left side give

$$-r^n\ln(1-\zeta)=C$$

or

$$\zeta=1-\exp(-Cr^{-n}) \quad (10)$$

This equation is valid when C_2S(ss) crystals with $0\leq Na/(Na+Ca)\leq 0.03$ are cooled at a constant rate from T_i to T_f.

In the present study all the C_2S(ss) samples were cooled from 1500℃, which exceeds the α-to-α'_H transition temperature, i.e., T_i. In our previous microscopic observations, the remelting reaction was almost completed before reaching 1200℃ (T_f).[4)] The temperature of quenching in the present experiment was 1000℃ and much lower than T_f.

From Eq. (10),

$$\ln\ln[1/(1-\zeta)]=\ln C-n\ln r \quad (11)$$

This equation gives a straight line when $\ln\ln[1/(1-\zeta)]$ is plotted against $\ln r$ (Fig. 4). The n value derived from the slope of the line is 0.25. The intercept of the line at $\ln r=0$ gives $\ln C=0.284$

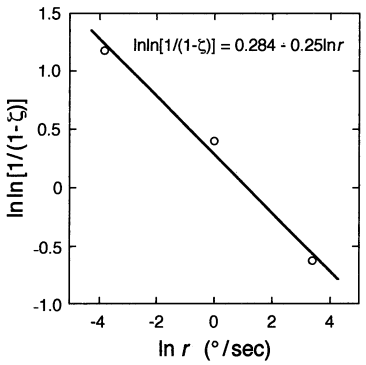

Fig. 4. Relationship between $\ln r$ and $\ln\ln[1/(1-\zeta)]$.

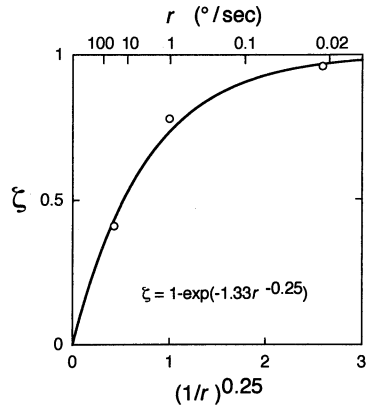

Fig. 5. The fraction remelted (ζ) as a function of cooling rate (r).

($C=1.33$). Figure 5 shows the relation between ζ and r, in which ζ increases steadily with decreasing r.

According to Christian,[14] the n value less than 1 corresponds to diffusion-controlled reactions. It is presumable, therefore, that the remelting reaction is diffusion controlled. Since the progress of the reaction was well represented by the decrease in the Na/(Na+Ca) ratio irrespective of the concentration of Al and Fe, the rate-determining step is presumably the bulk diffusion of Na atoms to the lamella boundaries to form exsolved liquid.

4. Conclusions

(1) With β-C_2S(ss) doped with Na_2O, Al_2O_3 and Fe_2O_3, the angle β varied sensitively with the Na/(Na+Ca) ratio.

(2) The change in impurity concentration caused by the remelting reaction of C_2S(ss) could best be followed by the change in the angle β.

(3) For C_2S(ss) with $0 \leq Na/(Na+Ca) \leq 0.03$ the fraction remelted was expressed by $1-\exp(-1.33\,r^{-0.25})$ with r as the cooling rate (°C/s).

Acknowledgment We thank Dr. Y. Kodama of the Ocean Research Institute, The University of Tokyo, for assistance in ICP analysis. This work was supported in part by funds from the Cooperative Program (No. 17) provided by the Ocean Research Institute.

References

1) H. F. W. Taylor, "Cement Chemistry", Academic Press (1990).
2) K. Fukuda, I. Maki, K. Toyoda and S. Ito, *J. Am. Ceram. Soc.*, **76**, 1821–24 (1993).
3) K. Fukuda, I. Maki and S. Ito, *J. Am. Ceram. Soc.*, **75**, 2896–98 (1992).
4) K. Fukuda, I. Maki, S. Ikeda and S. Ito, *J. Am. Ceram. Soc.*, **76**, 2942–44 (1993).
5) K. Fukuda, I. Maki, S. Ito, H. Yoshida and C. Kato, *J. Am. Ceram. Soc.*, **77**, 3027–29 (1994).
6) K. Fukuda and I. Maki, *Cem. Concr. Res.*, **19**, 913–18 (1989).
7) K. Fukuda and I. Maki, *Cem. Concr. Res.*, **23**, 599–602 (1993).
8) H. Toraya, *J. Appl. Crystallogr.*, **19**, 440–47 (1986).
9) A. Ghose and P. Barnes, *Cem. Concr. Res.*, **9**, 747–55 (1979).
10) A. C. Turnock, D. H. Lindsley and J. E. Grover, *Am. Mineral.*, **58**, 50–59 (1973).
11) M. Avrami, *J. Chem. Phys.*, **7**, 1103–12 (1939).
12) M. Avrami, *J. Chem. Phys.*, **8**, 212–24 (1940).
13) M. Avrami, *J. Chem. Phys.*, **9**, 177–84 (1941).
14) J. W. Christian, "The Theory of Transformations in Metals and Alloys", 2nd ed., Pergamon Press, Oxford (1975).